

Thermodynamics and heavy-quark free energies at finite temperature and density with two flavors of improved Wilson quarks

Y. Maezawa*, T. Hatsuda

*Department of Physics, The University of Tokyo,
Bunkyo-ku, Tokyo 113-0033, Japan
E-mail: maezawa@nt.phys.s.u-tokyo.ac.jp*

S. Aoki, K. Kanaya

*Graduate School of Pure and Applied Sciences, University of Tsukuba,
Tsukuba, Ibaraki 305-8571, Japan*

S. Ejiri

*Physics Department, Brookhaven National Laboratory,
Upton, New York 11973, USA*

N. Ishii, N. Ukita and T. Umeda

*Center for Computational Sciences, University of Tsukuba,
Tsukuba, Ibaraki 305-8577, Japan*

Thermodynamics of two-flavor QCD at finite temperature and density is studied on a $16^3 \times 4$ lattice, using a renormalization group improved gauge action and the clover improved Wilson quark action. In the simulations along lines of constant m_{PS}/m_V , we calculate the Taylor expansion coefficients of the heavy-quark free energy with respect to the quark chemical potential (μ_q) up to the second order. By comparing the expansion coefficients of the free energies between quark(Q) and antiquark(\bar{Q}), and between Q and Q , we find a characteristic difference at finite μ_q due to the first order coefficient of the Taylor expansion. We also calculate the quark number and isospin susceptibilities, and find that the second order coefficient of the quark number susceptibility shows enhancement around the pseudo-critical temperature.

*The XXV International Symposium on Lattice Field Theory
July 30 - August 4 2007
Regensburg, Germany*

*Speaker.

1. Introduction

We study QCD thermodynamics at finite temperature (T) and quark chemical potential (μ_q) with two-flavors of dynamical quarks. Then, we calculate the Taylor expansion coefficients of physical quantities in the simulations at $\mu_q = 0$, and investigate thermodynamic properties at small μ_q region. In this report, we present current status of two topics: heavy-quark free energy and fluctuation at finite μ_q . The former is related to the inter-quark interaction in quark-gluon plasma, and the latter is related to the existence of the critical point in (T, μ_q) plane.

2. Lattice action and simulation parameters

We employ a renormalization group improved gauge action and a clover improved Wilson quark action with two flavors. The numerical simulation is performed on a lattice with a size of $N_s^3 \times N_t = 16^3 \times 4$ along lines of constant physics, i.e. lines of constant m_{PS}/m_V (the ratio of pseudoscalar and vector meson masses) at $T = 0$ in the space of simulation parameters. Two values of m_{PS}/m_V are taken: 0.65 and 0.80 with the temperature range of $T/T_{pc} \sim 0.82$ –4.0 and 0.76–3.0, respectively, where T_{pc} is the pseudo-critical temperature along the line of constant physics. The number of trajectories for each run after thermalization is 5000–6000, and we measure physical quantities at every 10 trajectories. Details of the lines of constant physics with the same actions are summarized in Ref. [1, 2]. To calculate derivatives of the quark determinant with respect to μ_q , we use the random noise method introduced in Ref. [3] with the number of noise of 100–200.

3. Heavy quark free energy and Debye screening mass

The heavy-quark free energy in the QCD medium is one of the important quantities to characterize the properties of the quark-gluon plasma. Especially, the properties of the free energies at finite T and μ_q may be related to the fate of the charmoniums and bottomoniums in relativistic heavy ion collisions. Precise studies of the heavy-quark free energy in two-flavors QCD have been done with the improved Wilson quark action at $\mu_q = 0$ [2]. Properties of the free energy between static-quark (Q) and -antiquark (\bar{Q}) at finite μ_q have been previously investigated by using the Taylor expansion method using an improved staggered quark action [4]. In this section, we show the Taylor expansion coefficients of the free energy between not only Q and \bar{Q} , but also Q and Q , up to 2nd-order of μ_q .

The free energy of static quarks on the lattice is described by the correlations of the Polyakov loop: $\Omega(\mathbf{x}) = \prod_{\tau=1}^{N_t} U_4(\tau, \mathbf{x})$ where the $U_\mu(\tau, \mathbf{x}) \in \text{SU}(3)$ is the link variable. With an appropriate gauge fixing (e.g. the Coulomb gauge fixing), one can define the free energy in various color channels separately: the color singlet $Q\bar{Q}$ channel (**1**), the color octet $Q\bar{Q}$ channel (**8**), the color anti-triplet QQ channel (**3***), and the color sextet QQ channel (**6**), given as follows.

$$e^{-F^1(r,T)/T} = \frac{1}{3} \langle \text{Tr} \Omega^\dagger(\mathbf{x}) \Omega(\mathbf{y}) \rangle, \quad (3.1)$$

$$e^{-F^8(r,T)/T} = \frac{1}{8} \langle \text{Tr} \Omega^\dagger(\mathbf{x}) \text{Tr} \Omega(\mathbf{y}) \rangle - \frac{1}{24} \langle \text{Tr} \Omega^\dagger(\mathbf{x}) \Omega(\mathbf{y}) \rangle, \quad (3.2)$$

$$e^{-F^6(r,T)/T} = \frac{1}{12} \langle \text{Tr} \Omega(\mathbf{x}) \text{Tr} \Omega(\mathbf{y}) \rangle + \frac{1}{12} \langle \text{Tr} \Omega(\mathbf{x}) \Omega(\mathbf{y}) \rangle, \quad (3.3)$$

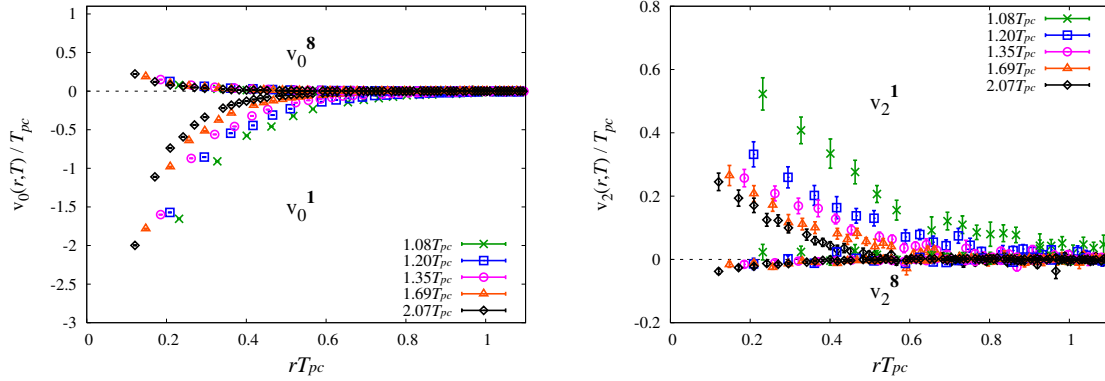


Figure 1: Results of v_0^M (left) and v_2^M (right) for $Q\bar{Q}$ channel above T_{pc} at $m_{PS}/m_V = 0.80$.

$$e^{-F^{3*}(r,T)/T} = \frac{1}{6} \langle \text{Tr} \Omega(\mathbf{x}) \text{Tr} \Omega(\mathbf{y}) \rangle - \frac{1}{6} \langle \text{Tr} \Omega(\mathbf{x}) \Omega(\mathbf{y}) \rangle, \quad (3.4)$$

where $r = |\mathbf{x} - \mathbf{y}|$.

For $T > T_{pc}$, we introduce normalized free energies (V^1, V^8, V^6, V^{3*}) such that they vanish at large distances. This is equivalent to define the free energies by dividing the right-hand side of Eq. (3.1)–(3.4) by $\langle \text{Tr} \Omega \rangle \langle \text{Tr} \Omega^\dagger \rangle$ for $Q\bar{Q}$ free energies and $\langle \text{Tr} \Omega \rangle^2$ for QQ free energies.

The Taylor expansion of normalized free energies with respect to μ_q/T is described as a power series up to 2nd order:

$$V^M(r, T, \mu_q) = v_0^M + v_1^M \left(\frac{\mu_q}{T} \right) + v_2^M \left(\frac{\mu_q}{T} \right)^2 + O(\mu_q^3), \quad (3.5)$$

where M is the color channel. The coefficients, v_n^M , can be evaluated by expanding the quark determinant of partition function in powers of μ_q , then the normalization of the free energies by $\langle \text{Tr} \Omega \rangle$ is also taken order by order of μ_q .

One should note that the color singlet and octet channels do not have the odd orders in the Taylor expansion since the free energies for both channels are symmetric with respect to μ_q . In other words, the free energies between Q and \bar{Q} are invariant under the charge conjugation. On the other hand, the color sextet and antitriplet channels has the odd orders since the QQ free energies are not invariant under the charge conjugation.

The expansion coefficients of the normalized free energies for the color singlet and octet $Q\bar{Q}$ channels are shown in Fig. 1 for v_0^M (left) and v_2^M (right) at $m_{PS}/m_V = 0.80$ for several temperatures. Those for the color sextet and antitriplet QQ channels are shown in Fig. 2 for v_0^M (left) and v_1^M (right) and in Fig. 3 for v_2^M . It have been found in Ref. [2] that the inter-quark interaction is “attractive” in the color singlet and antitriplet channels and is “repulsive” in the color octet and sextet channels at $\mu_q = 0$. We find that, both in high and low temperatures, the sign of v_1^M is the same with that of v_0^M , whereas the sign of a v_2^M is the opposite of that of v_0^M , i.e. $v_1^M \cdot v_0^M > 0$ (only for QQ free energies) and $v_2^M \cdot v_0^M < 0$. This means that the inter-quark interaction between Q and \bar{Q} becomes weak, whereas that between Q and Q becomes strong in the leading-order of μ_q . In other words, $Q\bar{Q}$ (QQ) free energies are screened (anti-screened) by contributions of the internal quarks induced by finite μ_q .

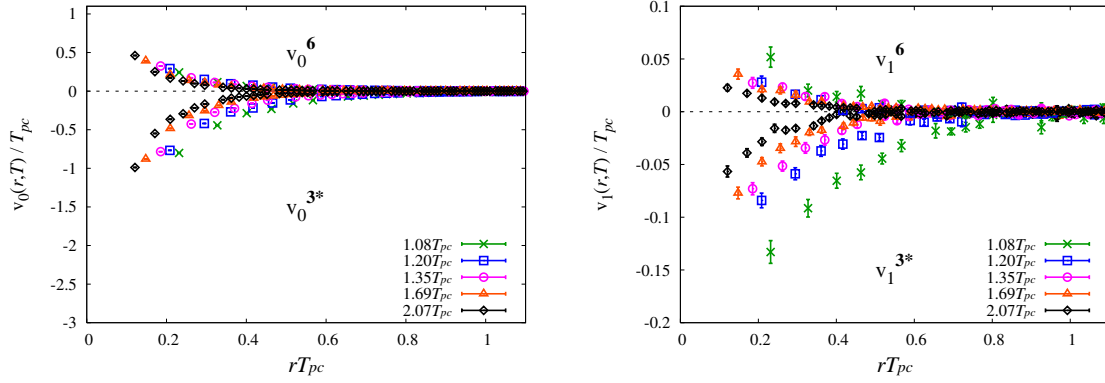


Figure 2: Results of v_0^M (left) and v_1^M (right) for QQ channel above T_{pc} at $m_{PS}/m_V = 0.80$.

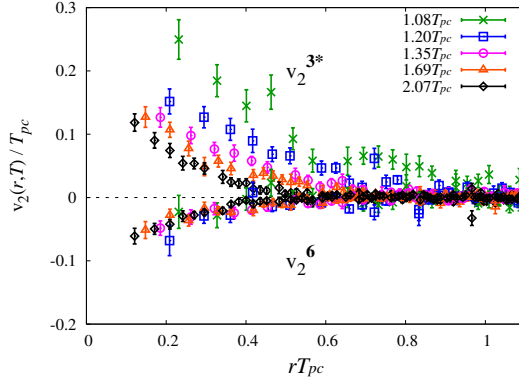


Figure 3: Results of v_2^M for QQ channel above T_{pc} at $m_{PS}/m_V = 0.80$.

In order to study the screening effect in each color channel, we fit the normalized free energies by a screened Coulomb form,

$$V^M(r, T, \mu_q) = C(M) \frac{\alpha_{\text{eff}}(T, \mu_q)}{r} e^{-m_D(T, \mu_q)r}, \quad (3.6)$$

where $\alpha_{\text{eff}}(T, \mu_q)$ and $m_D(T, \mu_q)$ are the effective running coupling and the Debye screening mass, respectively. We assume that contributions of finite μ_q appear only in α_{eff} and m_D . The Casimir factor $C(M) \equiv \langle \sum_{a=1}^8 t_1^a \cdot t_2^a \rangle_M$ for color channel M is given by

$$C(\mathbf{1}) = -\frac{4}{3}, \quad C(\mathbf{8}) = \frac{1}{6}, \quad C(\mathbf{6}) = \frac{1}{3}, \quad C(\mathbf{3}^*) = -\frac{2}{3}. \quad (3.7)$$

We assume that $m_D(T, \mu_q)$ is also expressed as a power series of μ_q/T :

$$m_D = m_{D,0} + m_{D,2} \left(\frac{\mu_q}{T} \right)^2 + O(\mu_q^4), \quad (3.8)$$

where we use the fact that the Debye screening mass does not have the odd powers in the Taylor expansion because it is related to the self-energy of the two-point correlation of the gauge fields which is symmetric when $\mu_q \rightarrow -\mu_q$. Relations of coefficients between V^M and m_D are given by comparing each order of μ_q . At $\mu_q = 0$, the relation is the same as that adopted in Ref. [2]:

$$v_0(r, T) = C(M) \frac{\alpha_{\text{eff},0}(T)}{r} e^{-m_{D,0}(T)r}. \quad (3.9)$$

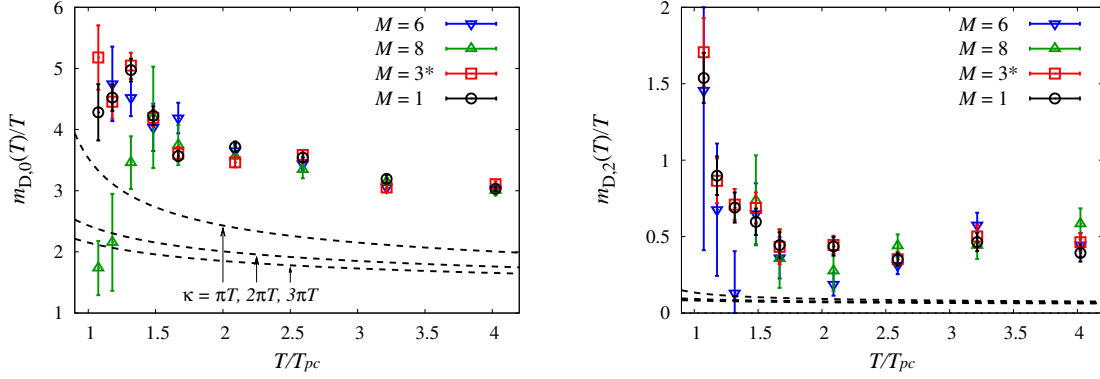


Figure 4: Results of $m_{D,0}$ (left) and $m_{D,2}$ for each color channel at $m_{PS}/m_V = 0.65$. Dashed lines are prediction from a leading-order of the thermal perturbation theory with the renormalization points of $\kappa = \pi T$, $2\pi T$ and $3\pi T$.

For the second order coefficients, we obtain,

$$\frac{v_2}{v_0} \simeq -m_{D,2} r. \quad (3.10)$$

At large distances, we estimate the coefficients of Debye mass by fitting the normalized free energies for each color channel with the formulae (3.9) and (3.10).

Figure 4 shows the results of the $m_{D,0}(T)$ (left) and $m_{D,2}(T)$ (right) for $m_{PS}/m_V = 0.65$. Similar behavior in both results are obtained for $m_{PS}/m_V = 0.80$. We find that there is no significant channel dependence in both coefficients at sufficiently high temperatures ($T \gtrsim 2T_{pc}$). In other words, the channel dependence of the free energy at high temperature can be well absorbed in the Casimir factor.

Let us compare the Debye screening mass at finite μ_q on the lattice with that predicted in the thermal perturbation theory. The 2-loop running coupling is given by

$$g_{2l}^{-2}(\kappa) = \beta_0 \ln \left(\frac{\kappa}{\Lambda} \right)^2 + \frac{\beta_1}{\beta_0} \ln \ln \left(\frac{\kappa}{\Lambda} \right)^2, \quad (3.11)$$

where κ is the renormalization point. The argument in the logarithms can be written as $\kappa/\Lambda = (\kappa/T)(T/T_{pc})(T_{pc}/\Lambda)$ with $\Lambda = \Lambda_{\overline{MS}}^{N_f=2} \simeq 261$ MeV [5] and $T_{pc} \simeq 171$ MeV [1]. We assume κ to be in a range πT to $3\pi T$. Therefore, g_{2l} can be viewed as a function of T/T_{pc} . In the leading order of the thermal perturbation theory, the Debye screening mass with g_{2l} is given by

$$m_D^{\text{LO}}(T, \mu_q) = g_{2l}(T) \left\{ \left(1 + \frac{N_f}{6} \right) T^2 + \frac{N_f}{2\pi^2} \mu_q^2 \right\}^{1/2}. \quad (3.12)$$

Therefore, the leading-order expansion coefficients in the thermal perturbation theory are given by

$$m_{D,0}^{\text{LO}}(T) = \sqrt{1 + \frac{N_f}{6}} g_{2l}(T) T, \quad m_{D,2}^{\text{LO}}(T) = \frac{1}{4\pi^2} \frac{N_f}{\sqrt{1 + N_f/6}} g_{2l}(T) T. \quad (3.13)$$

The dashed lines in Fig. 4 are the results of $m_{D,0}^{\text{LO}}$ and $m_{D,2}^{\text{LO}}$ for $\kappa = \pi T$, $2\pi T$ and $3\pi T$. We find that the lattice results are larger than the leading-order thermal perturbation for both coefficients

of the Debye mass. Since it is known that the next-to-leading-order in the thermal perturbation with respect to T compensates for such discrepancy in the case at $\mu_q = 0$ [2], the higher order contributions in the perturbation theory with respect to μ_q could help us to understand our results on the lattice.

4. Hadronic fluctuations at finite μ_q

Hadronic fluctuations at finite density are observables closely related to the critical point in the (T, μ_q) plane and may be experimentally detected by an event-by-event analysis of heavy ion collisions. The fluctuations can also be studied by numerical simulations of lattice QCD calculating the quark number and isospin susceptibilities, χ_q and χ_I . They correspond to the second derivatives of the pressure with respect to μ_q and μ_I , where μ_I is the isospin chemical potential. From a phenomenological argument in the sigma model, χ_q is singular at the critical point, whereas χ_I shows no singularity there [6].

In this section, we calculate the χ_q and χ_I and their second derivatives with respect to μ_q and μ_I at $\mu_q = \mu_I = 0$. (Note that the odd derivatives are zero at $\mu_q = 0$.) The details of the calculations are reported in Ref. [3]. The left panel of Fig. 5 shows χ_q/T^2 (circle) and χ_I/T^2 (square) at $m_{PS}/m_V = 0.8$ and $\mu_q = \mu_I = 0$ as functions of T/T_{pc} . We find that χ_q/T^2 and χ_I/T^2 increase sharply at T_{pc} , in accordance with the expectation that the fluctuations in the QGP phase are much larger than those in the hadron phase. Their second derivatives $\partial^2(\chi_q/T^2)/\partial(\mu_q/T)^2$ and $\partial^2(\chi_I/T^2)/\partial(\mu_q/T)^2$ are shown in Fig. 5 (right). We find that basic features are quite similar to those found previously with the p4-improved staggered fermions [7]. $\partial^2(\chi_I/T^2)/\partial(\mu_q/T)^2$ remains small around T_{pc} , suggesting that there are no singularities in χ_I at non-zero density. On the other hand, we expect a large enhancement in the quark number fluctuations near T_{pc} as approaching the critical point in the (T, μ_q) plane. The dashed line in Fig. 5 (right) is a prediction from the hadron resonance gas model, $\partial^2\chi_q/\partial\mu_q^2 \approx 9\chi_q/T^2$. Although current statistical errors in Fig. 5 (right) are still large, we find that $\partial^2(\chi_q/T^2)/\partial(\mu_q/T)^2$ near T_{pc} is much larger than that at high temperature. At the right end of the figure, values of free quark-gluon gas (Stefan-Boltzmann gas) for $N_f = 4$ and for $N_f = \infty$ limit are shown. Since the lattice discretization error in the equation of state is known to be large at $N_f = 4$ with our quark action, we need to extend our study to larger N_f for the continuum extrapolation.

5. Summary

We presented current status of thermodynamics of two-flavor QCD with the renormalization group improved gauge action and the clover improved Wilson quark action. Simulations were performed on a $16^3 \times 4$ lattice and along lines of constant $m_{PS}/m_V = 0.65$ and 0.80 .

The properties of the heavy-quark free energies at finite μ_q were studied in the Taylor expansion method up to 2nd order of μ_q . We find that there is a characteristic difference between $Q\bar{Q}$ and QQ free energies due to the first order coefficient of the Taylor expansion. It suggests that the inter-quark interaction between Q and \bar{Q} (Q and Q) become weak (strong) in the leading-order of μ_q . We also extract the expansion coefficients of the Debye screening mass for each color channel up to 2nd order of μ_q . The Debye mass shows no significant channel dependence at $T \gtrsim 2T_{pc}$, whereas,

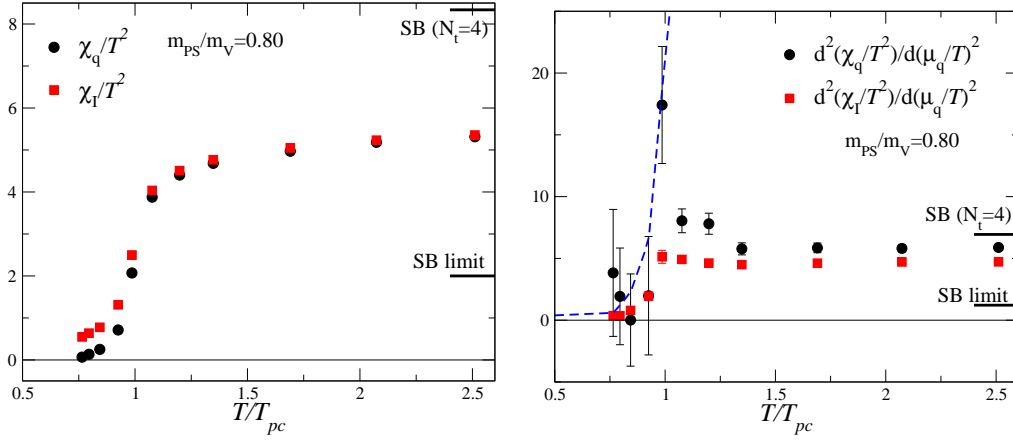


Figure 5: Left: Quark number (circle) and isospin (square) susceptibilities at $\mu_q = \mu_I = 0$. Right: The second derivatives of these susceptibilities.

we find disagreement with leading-order predictions of the thermal perturbation theory. Since it is known that the next-to-leading-order of the thermal perturbation with respect to T well reproduces the Debye mass on a lattice at $\mu_q = 0$ [2], the calculations of the higher order perturbation with respect to μ_q will help us to understand the results on the lattice.

The fluctuations of quark number and isospin densities were also discussed. Although the statistical errors are still large, we find that χ_q seems to increase rapidly near T_{pc} as μ_q increases, whereas the increase of χ_I is not large near T_{pc} . These behaviors qualitatively agree with the previous results obtained with the p4-improved staggered fermions.

Acknowledgements: This work is in part supported by Grants-in-Aid of the Japanese MEXT (Nos. 13135204, 15540251, 17340066, 18540253). YM is supported by JSPS, and SE is supported by the U.S. Department of Energy (DE-AC02-98CH1-886). This work is in part supported also by ACCC, Univ. of Tsukuba, and the Large Scale Simulation Program No.06-19 (FY2006) of KEK.

References

- [1] A. Ali Khan *et al.* (CP-PACS Collaboration), *Phys. Rev. D* **63** (2001) 034502; **64** (2001) 074510.
- [2] Y. Maezawa *et al.* (WHOT-QCD Collaboration), *Phys. Rev. D* **75**, (2007) 074501.
- [3] S. Ejiri *et al.* in proceedings of *Lattice 2006*, PoS (LAT2006) 132.
- [4] M. Döring, S. Ejiri, O. Kaczmarek, F. Karsch and E. Laermann, *Eur. Phys. J. C* **46**, 179 (2006).
- [5] M. Gockeler *et al.*, *Phys. Rev. D* **73** (2006) 014513.
- [6] Y. Hatta and M. A. Stephanov, *Phys. Rev. Lett.* **91** (2003) 102003.
- [7] C.R. Allton *et al.*, *Phys. Rev. D* **68** (2003) 014507; **71** (2005) 054508.